Density dependence of stopping cross sections measured in liquid ethane

Georg Both, Ralph Krotz, Karl Lohmer, and Wolfgang Neuwirth
Erstes Physikalisches Institut, Universität zu Köln, D-5000 Köln, Federal Republic of Germany
(Received 6 June 1983)

Electronic stopping cross sections for ^{7}Li projectiles (840—175 keV) have been measured with the inverted Doppler-shift attenuation method in liquid ethane (C_2H_6) at two different densities. The density of the target has been varied by changing the temperature, and measurements have been performed at 0.525 g/cm^3 (199 K) and 0.362 g/cm^3 (287 K). At the higher density the stopping cross section is about 2% smaller. This result agrees with a calculation of the stopping cross section of liquid ethane, applying Lindhard's theory in the local-density approximation using a simple model of the liquid. It is also in agreement with various observations of the so-called physical-state effect, which show that the stopping cross section of the same substance is smaller in a condensed phase than in the gaseous one.

I. INTRODUCTION

There is much experimental evidence for the "physical-state effect" in the electronic slowing down of ions. This means that in the velocity region around and below the maximum of energy loss the stopping cross section measured in a condensed target differs from that in a gas target for the same target compound. In Table I some results of measurements on this problem are displayed. A more detailed summary of the present knowledge of the physical-state effect is given by Thwaites.[1]

In most cases, the stopping cross sections in solids and liquids are smaller than in gases by about 5%. However, the physical-state effect cannot be explained by different charge states of the projectile in dense and gaseous media, because the projectile's charge seems to be almost the same in all target phases[2] or even larger in the dense ones.[3,4] Consequently, the physical-state effect results from properties of the target.

A high precision measurement (with an accuracy of about 1%) of the stopping cross section of one target compound in different phases using the same experimental device has not been performed up to now. This explains some discrepancies in Table I, because the systematic errors of individual experimental techniques may be underestimated. In Ref. 5 we described our observation that the nonmonotonic behavior of stopping cross sections in liquid *n*-alkanes is correlated with other properties depending on the intermolecular interaction. Similar correlations in the few available stopping cross sections for gaseous *n*-alkanes[6] could not be found. This is further confirmed by recent measurements by Baumgart *et al.*[7] of the stopping cross sections for the whole series of *n*-alkanes from methane to *n*-decane, using 60—700-keV protons and 100—1100-keV He projectiles. The observed deviations[5] of the individual stopping cross sections from their average values determined for the whole series of liquid *n*-alkanes are of the order of 1—2% of the molecular stopping cross sections. The absolute magnitude of the physical-state effect cannot be deduced from these data, but in any case it must be larger than these differences.

In order to obtain reliable information on the absolute magnitude of the physical-state effect, one must investigate the same target substance in different phases by the same accurate experimental procedure. Because our measuring method is not applicable for gaseous targets, we used an indirect method; we determined the stopping cross section of a liquid target at different densities. If the interaction between the atoms or molecules in the target is neglected, the stopping cross section $S=-N^{-1}dE/dx$, which is the differential energy loss $-dE/dx$ divided by the number density N in the target, would be independent of the target density. In reality, however, the average intermoleculear distances and the outer electron distribution of the molecules are correlated with the density. This affects the stopping cross section, not only in the case of the large density variation in the transition from the gaseous to the liquid state, but also if the density is varied in the liquid state. The corresponding change of the stopping cross section in the latter case can be detected if the experimental accuracy is high enough. We used liquid ethane (C_2H_6) as the target substance and varied its density by changing the temperature. The dependence of the density on the temperature is rather strong in ethane; the density may differ by almost a factor of 2 at two experimentally well accessible temperatures. A direct dependence of the stopping cross section on the temperature as recently calculated for plasmas[8] is negligible in our temperature range.

In Sec. II the experimental determination of the stopping cross sections of liquid ethane at 199 K and at 287 K is described. The results are compared in Sec. III with calculated values based on a simple model.

II. EXPERIMENTAL METHOD

The stopping cross section of liquid ethane has been measured via the inverted Doppler-shift attenuation method, which has been described in detail in Refs. 9 and 10. The Li projectiles are created inside the target by irradiation with thermal neutrons utilizing the reaction

$$^{10}\mathrm{B}(n_{\mathrm{th}},\alpha)^7\mathrm{Li}^* \ .$$

The Li nuclei are produced with a kinetic energy of 840

TABLE I. Experimental results concerning the physical-state effect. Highest density is hd; lowest density is ld.

Authors	Projectile energy (MeV)	Targets	Experimental device and accuracy	Result concerning the physical-state effect
Akhavan-Rezayat and Palmer[a]	He,1.0–8.0	Liquid and gaseous CH_3OH, C_3H_7OH, CH_2Cl_2, $CHCl_3$, CCl_4	Differentiation of range-energy curves, ~3%	$S_{liq.} < S_{gas.}$ 2–6% below 2 MeV
Matteson, Powers, and Chau[b]	He,0.3–2.0	H_2O ice H_2O vapor	Backscattering, ~4% Differentially pumped gas cell, ~1%	$S_{sol.} < S_{gas.}$ ~10% below 1 MeV
Thwaites[c]	He,0.3–5.5 1.8–4.8	H_2O vapor H_2O liquid	Differentiation of range-energy curves, 2–3%	$S_{liq.} < S_{gas.}$ ~4% down to 1.8 MeV
Chu, Braun, Davies, Matsunami, and Thompson[d]	He,0.5–2.0	Solid Ar, O_2, CO_2	Backscattering, 1–3%	$S_{sol.} < S_{gas.}$ (Refs. f,g) ~5% below 1 MeV
Besenbacher, Bøttiger, Graversen, Hansen, and Sørensen[e]	He,0.5–3.0	Solid Ar	Backscattering, ~3%	Agreement with Ref. d below 1 MeV
Chu and Powers[f]	He,0.3–2.0	Gaseous Ar and other gases	Differentially pumped gas cell, 1–2%	$S_{sol.}$ (Ref. d) $< S_{gas.}$ ~5% below 1 MeV
Bourland, Chu, and Powers[g]	He,0.3–2.0	Gaseous O_2, CO_2, and other gases	Differentially pumped gas cell, 1–2%	$S_{sol.}$ (Ref. d) $< S_{gas.}$ ~5% below 1 MeV
Besenbacher, Andersen, Hvelplund, and Knudsen[h]	He,0.1–2.4	Gaseous Ar, O_2, CO_2, and other gases	Differentially pumped gas cell, 1–2%	$S_{gas.} < S_{gas.}$ (Refs. f,g) up to 6%
Ziegler and Brodsky[i]	He,0.4–2.8	Amorphous Si, density varied by 5%	Backscattering, better than 1% (relative)	$S_{hd} < S_{ld}$ ~2%
Thwaites and Watt[j]	H,0–2 He,0–10	Gaseous and condensed targets	Survey of published data	$S_{cond.} < S_{gas.}$ ~15% at ~200 keV/amu

[a]A. Akhavan-Rezayat and R. B. J. Palmer, J. Phys. D 13, 1971 (1980).
[b]S. Matteson, D. Powers, and E. K. L. Chau, Phys. Rev. A 15, 856 (1977).
[c]D. I. Thwaites, Phys. Med. Biol. 26, 71 (1981).
[d]W. K. Chu, M. Braun, J. A. Davies, N. Matsunami, and D. A. Thompson, Nucl. Instrum. Methods 149, 115 (1978).
[e]F. Besenbacher, J. Bøttiger, O. Graversen, J. L. Hansen, and H. Sørensen, Nucl. Instrum. Methods 188, 657 (1981).
[f]W. K. Chu and D. Powers, Phys. Rev. B 4, 10 (1971).
[g]Reference 6.
[h]Reference 17.
[i]J. F. Ziegler and M. H. Brodsky, J. Appl. Phys. 44, 188 (1973).
[j]D. I. Thwaites and D. E. Watt, Phys. Med. Biol. 23, 426 (1978).

keV. The stopping time in the surrounding material is of the order of the lifetime (1.15×10^{-13} s) of the excited state at 478 keV; so, the shape of the corresponding γ line is Doppler-broadened and contains the information on the stopping power. The target substance needs a small amount of boron, which is added in form of a completely soluble boron compound.

This method is especially suited for liquid substances. Because of the starting velocity of the Li nuclei of $2.2v_B$ ($\approx$840 keV, v_B is Bohr's velocity which equals $e^2/\hbar=2.19\times10^6$ m/s), projectiles in the velocity range from $2.2v_B$ down to about $1v_B$ contribute to the measured Doppler-broadened γ spectrum. Assuming a linear dependence[9,10] of the stopping cross section on the projectile's velocity, we specify our stopping cross sections at v_B. Owing to the high penetrability of the 478-keV γ radiation and of thermal neutrons—producing the excited Li projectiles within the target—this experimental method allows also the investigation of liquefied gases inside a thick-walled container. A schematic sketch of our experimental setup is shown in Fig. 1. Neutrons from an Am/Be source are thermalized in water and paraffin. The cylindrical target vessel (with a volume of 2 l) surrounds a Ge(Li) detector measuring the Doppler-broadened γ spectrum and consists of an aluminum alloy, guaranteeing proper operation for pressures up to 45 bar in the temperature range from 100 to 400 K. For the whole setup, only materials could be used which have a small capture cross section for neutrons in order to minimize the background γ radiation. The temperature of the target is controlled by the level of a liquid coolant; the heat transfer is performed by a thick aluminum rod at the bottom of the target vessel. Four platinum resistors (Pt 100), fixed at different positions at the target, measure its temperature. The density of the target is calculated from these temperatures and known density data for ethane[11] in the vapor-liquid equilibrium and is corrected for the addition of the small amount of the boron compound [about 1 mol%, $B(OCH_3)_3$ at 287 K and a mixture[5] of $B(OCH_3)_3$ and ethanol at 199 K].

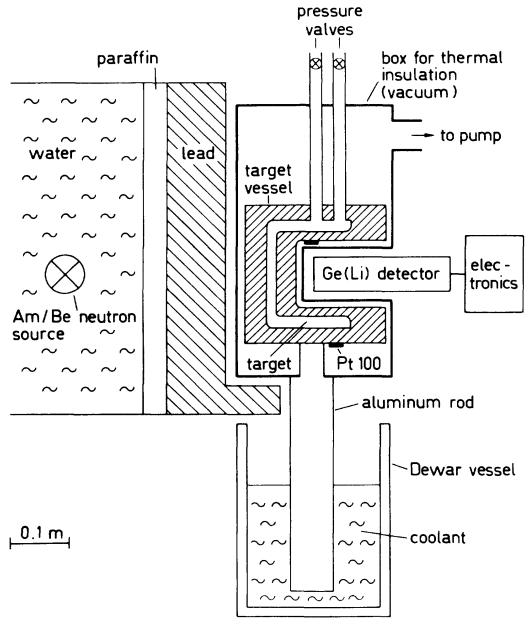

FIG. 1. Experimental device for the measurement of the stopping cross section of liquid ethane at different temperatures.

The desired precision for the result of the stopping cross section at a given temperature requires a total data collecting time of about 100 h. In order to avoid errors arising from drifts in temperature, single measurements with periods from 2.5 to 11 h were performed. The single values are statistically distributed around the mean value. The total error of the results consists of the statistical error and the error of the density, which has about the same magnitude. A systematic error due to the error of the lifetime of the excited state at 478 keV has not been included.[10] In Table II the results for the stopping cross sections of ethane at 199 and 287 K are presented.

III. DISCUSSION

The present experimental result (Table II) supports the general trend of the data in Table I: the higher the target density, the lower the stopping cross section. As outlined in Sec. I, this cannot be explained by different projectile charges. Our result is thus a consequence of target structure. In the dielectric theory of energy loss all relevant target properties are comprised within the dielectric function. For any targets, however, this function is not completely known in the necessary frequency region. So we apply Lindhard's theory[12] for the free-electron gas (including Lindhard's dielectric function) in the local-density approximation[13–15] in order to estimate the stopping cross section of liquid ethane. The electron distribution of the ethane molecule at different target densities is estimated with a simple model of a molecule in a liquid.

In the local-density approximation, the stopping cross section of a target atom or molecule with electron density $n(\vec{r})$ is

$$S(v)=\frac{4\pi e^4}{mv^2}Z_{1\text{eff}}^2(v)\int n(\vec{r})L[n(\vec{r}),v]dV\ . \tag{1}$$

TABLE II. Experimental stopping cross sections of liquid ethane at two different densities for ^{7}Li projectiles at Bohr's velocity in atomic units (1 a.u. $=0.762\times10^{-15}$ eV cm^2).

Temperature (K)	Density (g/cm^3)	Stopping cross section
199	0.525	163.5±1.4
287	0.362	166.5±1.5
Difference:		3.0±2.0 (1.8±1.2)%

Here e and m are charge and mass of the electron, v is the projectile's velocity, and L is Lindhard's stopping function. The integration is performed over the volume of one target atom or molecule. As a further approximation, the effective projectile charge[15,16,4] $Z_{1\text{eff}}$ has been used, which depends on the projectile's velocity only. A 1% accuracy can certainly not be achieved with Eq. (1), because Z_1^3 and Z_1^4 terms[17] are not included and because the concept of effective charge[17] as well as the local-density approximation[14,15] are subject to larger uncertainties. Nevertheless, Eq. (1) has been applied by several authors, who compared their calculations with experiment: Land *et al.*[18] reproduced the Z_2 oscillations for 100-keV ^{7}Li ions ($0.76v_B$) with an accuracy of 10%. Iafrate *et al.*[14] used solid-state electron densities; for a projectile velocity of $2.0v_B$ deviations from experimental data up to 30% were found. Gertner *et al.*[19] applied Eq. (1) with the solid-state charge densities calculated by them; they reached an accuracy of about 10% for projectile velocities of $2.0v_B$ and $2.8v_B$. These comparatively large errors refer to the absolute magnitude of the stopping cross section. But as we want to compare the stopping cross sections of ethane in slightly different states only, the systematic errors implied in Eq. (1) are approximately the same in both cases.

The stopping function $L(n,v)$ as a function of n (above 10^{22} cm^{-3}) has been evaluated down to a projectile energy of 100 keV/amu ($v=2.008v_B$) by Iafrate and Ziegler.[20] In Eq. (1) we use this $L(n,2.008v_B)$ for electron densities above 10^{22} cm^{-3}. Below $n=10^{22}$ cm^{-3} we apply an approximation[13] for L which is valid in the case $v\gg v_F=(\hbar/m)(3\pi^2n)^{1/3}$. At $n=10^{22}$ cm^{-3} both values of L differ only slightly. Because in the velocity region $v_B<v<2v_B$ the stopping power depends linearly on v, we use Eq. (1) to calculate $S(2.008v_B)$ and obtain

$$S(v_B)=\frac{v_B}{2.008v_B}S(2.008v_B)\ . \tag{2}$$

The electron density $n(\vec{r})$ of an ethane molecule in the liquid can be estimated in the following simple way. In the first step the stopping cross section of a free ethane molecule (C_2H_6) is approximated[21] by

$$S(C_2H_6)=6[(1-i)S(H)+iS(H^+)]+2[(1-3i)S(C)+3iS(C^-)]\ . \tag{3}$$

Here $S(H)$, $S(C)$, $S(H^+)$, and $S(C^-)$ are the stopping cross sections of hydrogen and carbon atoms and ions; $S(H^+)=0$. The C—H bond is polar with a fraction i.

From the difference of electronegativity between carbon and hydrogen it follows $i=0.04$, according to Pauling.[22] It is known, however, that bonds involving excited configurations (as those of sp^3-hybridized carbon) have a smaller ionic character.[23] Therefore, we put $i=0$ (i is small, in any case) and Eq. (3) is replaced by

$$S(C_2H_6)=2S(C)+6S(H) . \quad (4)$$

Now $S(C)$ and $S(H)$ can be evaluated via Eq. (2), using atomic wave functions of free atoms to calculate the electron densities. To account for the bond structure in ethane (besides the consideration of i), we apply wave functions[24] yielding the electron density of the sp^3-hybridized carbon atom. In this case, the electron densities of hydrogen and carbon are spherically symmetric, which facilitates the numerical integration in Eq. (1).

In the second step we examine how the electron densities of hydrogen and carbon change, when the ethane molecule is surrounded by other ethane molecules in the liquid. In this case, each molecule is confined to a finite volume V_E. The average value for V_E follows from the density[11] ρ_E of the liquid

$$V_E=A_E/(N_A\rho_E) ,$$

where A_E is the molecular weight of ethane and N_A is Avogadro's constant. Because of its hexagonal structure we have centered each ethane molecule in a hexagonal prism with volume V_E (Fig. 2); the whole volume of the liquid can be completely filled with such prisms. The distance R between each hydrogen nucleus and the nearest surface of the prism can be calculated from V_E, the bond lengths, and the bond angles. In order to correlate uniquely each electron with its molecule, we modify the charge densities of the hydrogen atoms so that they are zero outside their own prisms. The simplest way to achieve this is to replace $n_{H,free}(r)$ by

$$n_{H,cutoff}(r)=\begin{cases} n_{H,free}(r), & r\le R_1 \\ n_{H,free}(R_1), & R_1\le r\le R \\ 0, & r>R . \end{cases}$$

If R is given, R_1 follows from the conservation of charge

$$\int_0^\infty n_{H,cutoff}(r)4\pi r^2dr=\int_0^{R_1} n_{H,free}(r)4\pi r^2dr + n_{H,free}(R_1)\int_{R_1}^{R} 4\pi r^2dr=1 .$$

In order to evaluate the stopping cross section of one ethane molecule in the liquid, $S(H)$ in Eq. (4) is replaced by $S(H_{cutoff})$, where $S(H_{cutoff})$ has been calculated via Eq. (2) using $n_{H,cutoff}(r)$ instead of the free atom's charge density.

The hydrogen electron distributions have been restricted too much, because only a part of them is directed to the prism's surface. This overestimates the contribution of the six hydrogen atoms to the physical-state effect, which, however, can be compensated by disregarding a similar cutoff procedure for the eight outer electrons of the two carbon atoms. As the cutoff radius R is determined by the average density ρ_E, this picture considers the liquid as completely filled with the corresponding regular prisms.

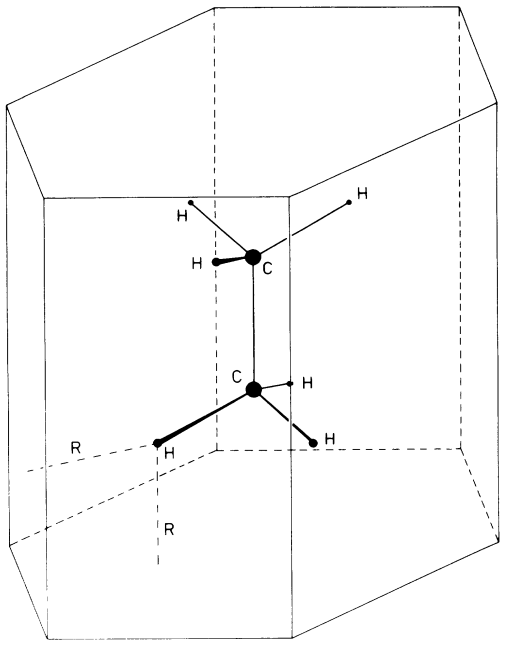

FIG. 2. An ethane molecule centered in a hexagonal prism. R is the distance between each H nucleus and the nearest surface of the prism. Bond lengths (Ref. 25): C—C, 1.5326±0.0020 Å; C—H, 1.1108±0.0020 Å. Bond angle (Ref. 25) H—C—H: 107.3°±0.3°.

This certainly does not supply a detailed description of the liquid state, because the decrease of density in a liquid is mainly caused by the decrease of the average number of the nearest neighbors of an arbitrarily chosen molecule rather than by the increase of intermolecular distances.[26] For our purpose, however, the use of distorted polyhedrons—representing the real situation in the liquid—instead of regular prisms seems not to be necessary. Because, in order to estimate how the compression of the electron distribution of an atom or a molecule influences the stopping power, the consideration of an average case is sufficient.

Finally, the argument given in the discussion of the applicability of Eq. (1) holds here too: We are interested in the small difference between the stopping cross sections of liquid ethane at two different densities only. Thus systematic errors of our model should be less important.

Table III gives the stopping cross sections of liquid ethane at 199 and 287 K calculated in the way described. The factor $Z_{1eff}(2.008v_B)$ has been fitted to the experimental point at 287 K; its value is 1.87 which is compatible with the effective charge given in Ref. 4. For compar-

TABLE III. Stopping cross sections $S(C_2H_6)$ of one ethane molecule for ^{7}Li projectiles at Bohr's velocity, calculated as described in the text. 1 a.u. $=0.762\times10^{-15}$ eV cm^2.

State	$S(C_2H_6)$ (a.u.)
Free molecule	170.6
Liquid (287 K)	166.5
Liquid (199 K)	163.8
Solid (77 K)	159.1

ison, the stopping cross sections of solid ethane (calculated using the density of solid ethane[27] at 77 K) and of gaseous ethane (calculated using $n_{H,free}$ instead of $n_{H,cutoff}$) are also given. The difference between the calculated stopping cross sections at 199 and 287 K (2.7 a.u.) agrees well with that of the measured values (3.0±2.0 a.u.).

IV. CONCLUSION

We have measured the stopping cross section of liquid ethane at two different densities. Our observation that the stopping cross section at the higher density is (1.8±1.2)% lower than at the lower density must be related to the physical-state effect. Many properties of a liquid are determined by intermolecular forces. The influence of the intermolecular interaction[5] on stopping cross sections can be understood in the following way: Intermolecular forces cause the phase transition from a gas to a liquid. This leads to a redistribution of the electrons. The main effect on the stopping cross section results from the confinement of the electron distributions of the individual molecules to a finite volume. A simple model of a liquid based on this description (applying Lindhard's theory in the local-density approximation) can be used to calculate the variation of stopping cross section with the density.

Extrapolations to the solid-state and the gaseous phase of ethane, the latter must be considered with some caution, yield a total difference in the stopping cross sections of 7% in good agreement with previous results on the physical-state effect (see Table I).

The density of a liquid can be changed not only by varying the temperature and pressure, but also by changing the concentration in an appropriate mixture. In a subsequent paper we shall report on measurements in such systems and their relation to the physical-state effect.

ACKNOWLEDGMENT

The financial support by the Bundesminister für Forschung und Technologie is gratefully acknowledged.

[1]D. I. Thwaites, Radiat. Res. (in press).
[2]J. M. Anthony and W. A. Lanford, Phys. Rev. A 25, 1868 (1982).
[3]N. Bohr and J. Lindhard, K. Dan. Vidensk. Selsk. Mat.-Fys. Medd. 28, No. 7 (1954).
[4]W. Brandt, Nucl. Instrum. Methods 194, 13 (1982).
[5]G. Both, R. Kreutz, R. Krotz, K. Lohmer, and W. Neuwirth, Phys. Rev. A 24, 1713 (1981).
[6]P. D. Bourland, W. K. Chu, and D. Powers, Phys. Rev. B 3, 3625 (1971); A. S. Lodhi and D. Powers, Phys. Rev. A 10, 2131 (1974).
[7]H. Baumgart (unpublished).
[8]N. R. Arista and W. Brandt, Phys. Rev. A 23, 1898 (1981); T. A. Mehlhorn, J. Appl. Phys. 52, 6522 (1981); K. A. Brueckner, L. Senbetu, and N. Metzler, Phys. Rev. B 25, 4377 (1982).
[9]W. Neuwirth, U. Hauser, and E. Kühn, Z. Phys. 220, 241 (1969); U. Hauser, W. Neuwirth, W. Pietsch, and K. Richter, *ibid.* 269, 181 (1974).
[10]R. Kreutz, W. Neuwirth, and W. Pietsch, Phys. Rev. A 22, 2598 (1980).
[11]L. A. Weber, J. Chem. Phys. 65, 446 (1976); D. R. Douslin and R. H. Harrison, J. Chem. Thermodyn. 5, 491 (1973); P. Sliwinski, Z. Phys. Chemie Neue Folge 63, 263 (1969). The densities given in these references agree within 0.2%.
[12]J. Lindhard and A. Winther, K. Dan. Vidensk. Selsk. Mat.-Fys. Medd. 34, No. 4 (1964).
[13]I. Gertner, M. Meron, and B. Rosner, Phys. Rev. A 18, 2022 (1978).
[14]G. J. Iafrate, J. F. Ziegler, and M. J. Nass, J. Appl. Phys. 51, 984 (1980).
[15]J. F. Ziegler, Nucl. Instrum. Methods 168, 17 (1980).
[16]P. Mertens and T. Krist, Nucl. Instrum. Methods 168, 33 (1980); B. S. Yarlagadda, J. E. Robinson, and W. Brandt, Phys. Rev. B 17, 3473 (1978); J. F. Ziegler, Nucl. Instrum. Methods 149, 129 (1978); J. F. Ziegler, Appl. Phys. Lett. 31, 544 (1977); R. K. Nesbet and J. F. Ziegler, *ibid.* 31, 810 (1977).
[17]F. Besenbacher, H. H. Andersen, P. Hvelplund, and H. Knudsen, K. Dan. Vidensk. Selsk. Mat.-Fys. Medd. 40, No. 3 (1979).
[18]D. J. Land, J. G. Brennan, D. G. Simons, and M. D. Brown, Phys. Rev. A 16, 492 (1977).
[19]I. Gertner, M. Meron, and B. Rosner, Phys. Rev. A 21, 1191 (1980).
[20]G. J. Iafrate and J. F. Ziegler, J. Appl. Phys. 50, 5579 (1979).
[21]W. Neuwirth, W. Pietsch, and R. Kreutz, Nucl. Instrum. Methods 149, 105 (1978).
[22]L. Pauling, *The Nature of the Chemical Bond,* 3rd ed. (Cornell University Press, Ithaca, New York, 1960).
[23]J. March, *Advanced Organic Chemistry: Reactions, Mechanisms and Structure* (McGraw-Hill, Kogakusha, Tokyo, 1968), p. 18.
[24]W. L. Luken and O. Sinagoğlu, At. Data Nucl. Data Tables 18, 525 (1976).
[25]J. H. Callomon, E. Hirota, K. Kuchitsu, W. J. Lafferty, A. G. Maki, C. S. Pote, *Structure Data of Free Polyatomic Molecules,* Vol. 7/Group II of *Numerical Data and Functional Relationships in Science and Technology, Landolt-Börnstein, New Series,* edited by K.-H. Hellwege (Springer, Berlin, 1976), p. 196.
[26]See, e.g., H. S. Green, in *Encyclopedia of Physics,* edited by S. Flügge (Springer, Berlin, 1960), Vol. X.
[27]J. W. Stewart and R. I. LaRock, J. Chem. Phys. 28, 425 (1958).